DETERMINATION OF COSMOLOGICAL PARAMETERS BY COSMIC MICROWAVE BACKGROUND

NAOSHI SUGIYAMA
Department of Physics, Kyoto University
Kyoto 606-01, Japan

1. Introduction

After the sensational discovery of Cosmic Microwave Background (CMB) anisotropies by Differential Microwave Radiometer (DMR) boarded on the Cosmic Background Explore (COBE) (Smoot et al. 1992), the number of observational data of temperature fluctuations have been rapidly increasing (see e.g., White, Scott and Silk 1994) together with the understanding of physical processes of evolution of CMB anisotropies. Nowadays, CMB anisotropies are becoming one of the key observational object in the modern cosmology. CMB anisotropies provide us direct information at last scattering surface, i.e., redshift $z \approx 1000$. Since the shape of the angular power spectrum of CMB anisotropies is highly sensitive to geometry of the universe, cosmological models and cosmological parameters, i.e., density parameter Ω_0, Hubble constant h which is normalized by 100km/s/Mpc, cosmological constant Λ, baryon density Ω_B and so on, CMB anisotropies are expected to be a new tool to understand our universe. Moreover, we can obtain information of thermal history of the universe after recombination (through the formation of secondary fluctuations and damping of primary fluctuations), physics of clusters of galaxies (through the Sunyaev-Zeldovich effect) and non-linear structure of the universe (through the gravitational lensing effect) from CMB anisotropies.

2. Primary CMB Anisotropies

The modern cosmology tells us that the inflation in the very early stage of the universe produced the seeds of fluctuations both on the matter densities and radiation densities. Matter density fluctuations grew to be the

K. Sato (ed.), Cosmological Parameters and the Evolution of the Universe, 88–97.

large scale structure of the universe such as galaxies, clusters of galaxies, super-clusters and so on. On the other hand, Photon density fluctuations are observed as temperature anisotropies in CMB. In addition to these primary anisotropies, there are several secondary fluctuations which are produced after the recombination as mentioned in the previous section. Among them, the Sunaev-Zeldovich effect is the important secondary effect since we can determine the distance (and the Hubble constant) to the cluster by this effect. And the possible existence of significant reionization of the universe after recombination becomes the biggest loophole to determine the cosmological parameter by using CMB anisotropies. In this paper, however, we restrict on primary anisotropies.

For the reason of simplicity, we treat density perturbations in the Fourier space. The temperature fluctuation Θ is defined as the energy integral of the linear perturbation of the temperature distribution function. We expand it into multipole components ℓ as

$$\Theta(\eta, \mu, k) = \sum_{\ell} (-i)^{\ell} \theta_{\ell}(k, \eta) P_{\ell}(\mu), \tag{1}$$

where η is conformal time, μ is direction cosign, P_{ℓ} is the Legendre polynomial. In order to get expected CMB anisotropies for each models with different cosmological parameters, we have to solve the Boltzmann equation for Θ. As end results, we get the temperature power spectrum in ℓ space as

$$\frac{2\ell+1}{4\pi} C_{\ell} = \frac{V}{2\pi^2} \int \frac{dk}{k} \frac{k^3 |\theta_{\ell}|^2}{2\ell+1} . \tag{2}$$

There are several efforts to solve the equation numerically (see e.g., Sugiyama 1995). It is possible to get C_{ℓ} in high accuracy from the numerical calculation. Although this procedure itself is perfectly reasonable, the final power spectrum contains a lot of different physical processes and it is very hard to separate each effects numerically. In order to get physical insight, we further developed a toy model based on the analogy of a harmonic oscillator (Hu, Sugiyama & Silk 1997). In this paper, we explain the dependence of CMB anisotropies on cosmological parameters by using this toy model. Throughout this paper, we employ cold dark matter (CDM) models as an example. Applications to other models are rather straight forward.

3. Physical Processes

By developing an analytic treatment for evolution of CMB anisotropies, we succeed to divide physical mechanism of evolution of CMB anisotropies into individual processes (see e.g., Hu & Sugiyama 1995a,b) as follows. (a)Acoustic oscillations: Before the recombination, photons and baryons

are tightly coupled each other. Once fluctuations cross the sound horizon, fluctuations of this tight coupled fluid oscillate as acoustic waves. These acoustic oscillations create peaks and wriggles on the power spectrum. Peaks are generated by not velocity fluctuations but density fluctuations. Therefore the naming of 'Doppler peak' is misleading. We would like to call them as 'Acoustic peaks'. (b)Diffusion Damping: Random walk of photons causes the exponential damping on fluctuations (Silk 1968). The damping length is smaller than the sound horizon before the recombination. During the recombination process, however, the damping length grows to infinity. On the other hand, the scattering probability between photons and baryons decreases and becomes negligibly small right after the recombination. Eventually the total damping rate becomes smaller on larger scales. (c)Gravitational redshift: After recombination, the coupling between photons and baryons are cut off. Without getting further scattering unless reionization of the vast region of the universe happens, temperature perturbations freely stream toward us. Photon perturbations are only disturbed by the gravitational potential. Climbing up the gravitational well, photons loose energy and are redshifted. This redshift effect caused by the gravitational potential at the recombination (last scattering surface) is called as the Sachs-Wolfe (SW) effect (Sachs & Wolfe 1967). For adiabatic perturbations, Gravitational potential stays constant during pure matter or radiation dominated regime in the flat $\Omega_0 = 1$ universe. However, it decays if one of these assumptions are broken. The decay of the gravitational potential also causes the redshift (or rather blue-shift) of photons. Here we refer to this effect as the Integrated Sachs-Wolfe (ISW) effect. The ISW contribution is separated into two parts. Right after the recombination, if the universe is still not purely matter dominated, the potential decays. We call this as the early ISW effect. It should be noticed that this effect is important even for the 'standard' model with $\Omega_0 = 1$ and $h = 0.5$. In case of the low density universe, the potential starts to decay very near present epoch when the curvature or the cosmological constant starts to become the dominant component. We refer to this effect as the late ISW effect. (d)Doppler effect: If the baryon velocity is different from photon's, the baryon velocity induces temperature fluctuations. During the tight coupling regime, baryon and photon velocities are identical. If the universe is transparent, there is no interaction between photons and baryons. Therefore this effect only appears in late time reionized models.

Our analogy of a harmonic oscillator is shown in figure 1. Balls connected by a spring are set inside the gravitational well. The deviation of the balls' location from the center of the oscillation corresponds to the amplitude of the fluctuations. The spring represents the pressure. The initial location is specified by the initial condition, i.e., adiabatic or isocurvature

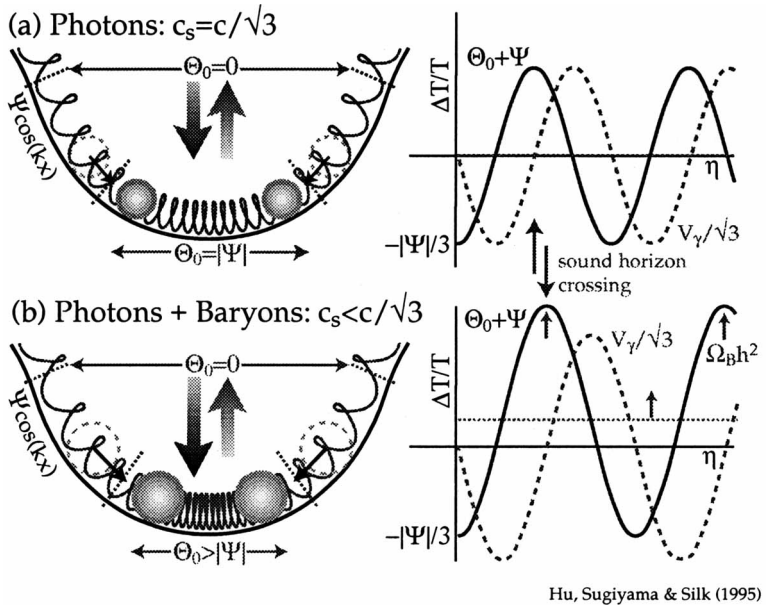

Figure 1. A toy model of the acoustic oscillation. Θ_0 is temperature fluctuations, Ψ is gravitational potential, V_γ is velocity perturbations of photons, c_s is sound peed and c is the speed of light. (a): low Ω_B limit, i.e., $c_s^2 = c^2/3$. (b): high Ω_B. This figure is reprinted from Hu, Sugiyama & Silk (1995).

conditions. Balls are kept at this initial location until fluctuations cross the sound horizon. Once crossing the sound horizon, they start to oscillate. At the recombination epoch, all oscillations are frozen out. They climb up the potential well to transfer to observers at present. If fluctuations of which wave length is larger than the sound horizon at last scattering surface are considered, balls stay at initial location until recombination epoch. Assuming matter domination epoch, we get the location as $-(2/3)\Psi$ for adiabatic perturbations. Here Ψ is the gravitational potential. The redshift effect caused by climbing up the well is Ψ. Therefore we get the famous Sachs-Wolfe value $\Psi/3$ for long wave length fluctuations. Next let us consider shorter wave length fluctuations. The recombination occurs after oscillation starts. A first compression mode at the last scattering surface corresponds to the first peak, a first depression mode corresponds to the second peak and so on.

https://doi.org/10.1017/S0074180900132206 Published online by Cambridge University Press

4. Shape of CMB Spectrum

Using our simple analytic picture, we can easily explain the dependence of CMB spectrum on various cosmological parameters. First, we investigate the height of the peaks. General statements are followings. Pressure of photon-baryon fluid prevents fluctuations from growth. Hence less pressure (which corresponds to heavier balls in our analogy) means higher peaks. On the other hand, Gravitational potential induces adiabatic growth. This causes blue-shift. Deeper potential seems to generate higher peaks. However, deeper potential well means bigger SW effect which causes redshift. Therefore deeper potential doesn't necessarily produce higher peaks. It is known that the gravitational potential decays if fluctuations cross the horizon during radiation dominated era. This decay boosts acoustic oscillations. First reason of this boost is because of resonant oscillation since the decay of potential approximately synchronizes with the cycle of acoustic oscillations. Second reason is the time dilation effect. Gravitational potential stretches the geometry and causes time delay, i.e., redshift on CMB anisotropies. As potential decays, photons get blue-shifted. Eventually, the shallower (deeper) potential makes peaks higher (lower).

How about the dependence of each cosmological parameters? If we consider $\Omega_B = 0$ limit, the sound speed is $c/\sqrt{3}$ where c is the speed of light. In this case, the amplitudes of density and velocity peaks are identical (see Fig.1 (a)). Therefore there is no peak in C_ℓ simply because density and velocity perturbations are $\pi/2$ off phase. Let us consider more realistic case. The sound speed is always smaller than $c/\sqrt{3}$ if we take into account the baryon density. Increasing $\Omega_B h^2$ decreases the sound speed. Hence we can expect higher peaks (See Fig.1 (b)). Increasing $\Omega_0 h^2$ pushes the matter-radiation equality earlier. This causes potential to be deeper and peaks to be lower.

We can explain most of parameter dependence from above arguments. For example, if we increase Ω_B with fixing Ω_0 and h, the sound speed becomes smaller. Therefore we get larger peaks as shown in figure 2 (a). Because above two effects compensate each other, h dependence with fixing Ω_B and Ω_0 is complicated. However, if we fix $\Omega_B h^2$ which is determined by BBN, increasing h simply provides lower peaks (see figure 2 (b)).

Secondly we show dependence of the location of peaks on cosmological parameters. The peak location is determined by the projection of the sound horizon at last scattering surface into observed angle. Because the sound horizon is a weak function of $\Omega_B h^2$, the peak location is almost independent on Ω_B and h. On the other hand, it strongly depends on Ω_0. The low density universe has longer age. Therefore the last scattering surface is further than the one of the high density universe. This effect makes the

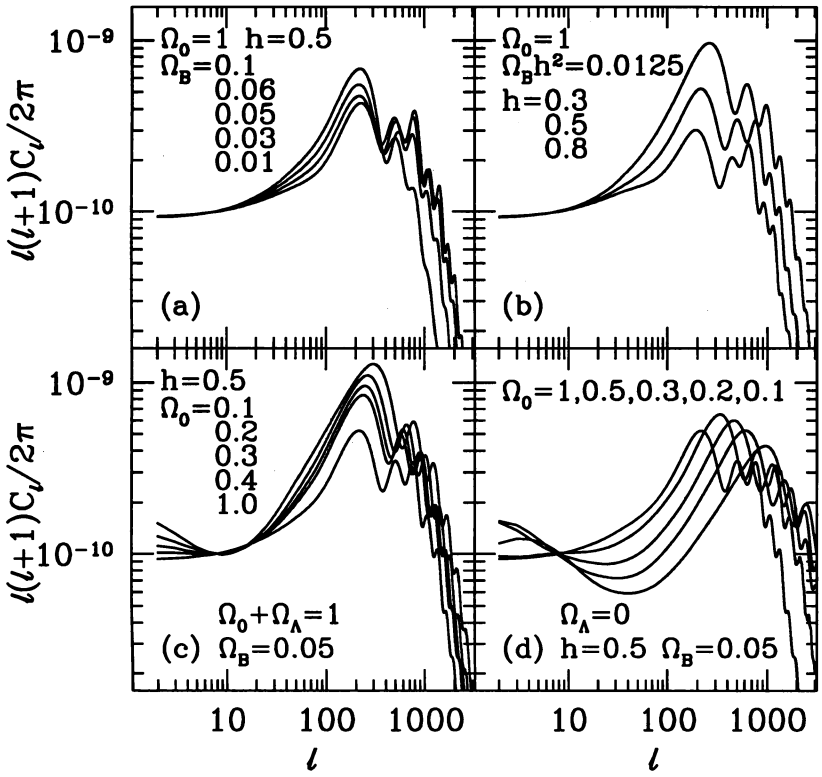

Figure 2. Cosmological parameter dependence of CMB power spectrum C_ℓ's as function of multipole ℓ. C_ℓ's are normalized to COBE-DMR 2 year data. Panel (a) shows Ω_B dependence with fixing Ω_0 and h. From the top to the bottom, $\Omega_B = 0.1, 0.06, 0.05, 0.03$ and 0.01. Panel (b) is h dependence with fixing $\Omega_B h^2$. From the top to the bottom, $h = 0.3, 0.5$ and 0.8. Panel (c) and (d) show Ω_0 dependence for flat cosmological constant dominated models and open models, respectively. From the top to the bottom of panel (c), $\Omega_0 = 0.1, 0.2, 0.3, 0.4$ and 1.0. From the left to the right of the first peak location of panel (d), $\Omega_0 = 1.0, 0.5, 0.3, 0.2$ and 0.1. For open models (panel (d)), we assume the flat potential power spectrum for the shape of the initial power spectrum which is predicted by open inflationary models (Lyth and Stwart 1990, Ratra and Peebles 1995).

sound horizon correspond to the smaller angular scale. Moreover, in the open universe, there is a geodesic effect which causes the same but bigger effect (Kamionkowski, Sugiyama & Spergel 1994). As is shown in figure 2 (c) and (d), peak locations are placed in order of $\Omega_0 = 1$, Λ and open models from large to small scales.

Finally, we would like to mention the peculiar behaviour of CMB power spectrum on large scales (small ℓ) for low density models which is shown in figure 2 (c) and (d). On large scales, the SW effect which produces the flat

https://doi.org/10.1017/S0074180900132206 Published online by Cambridge University Press

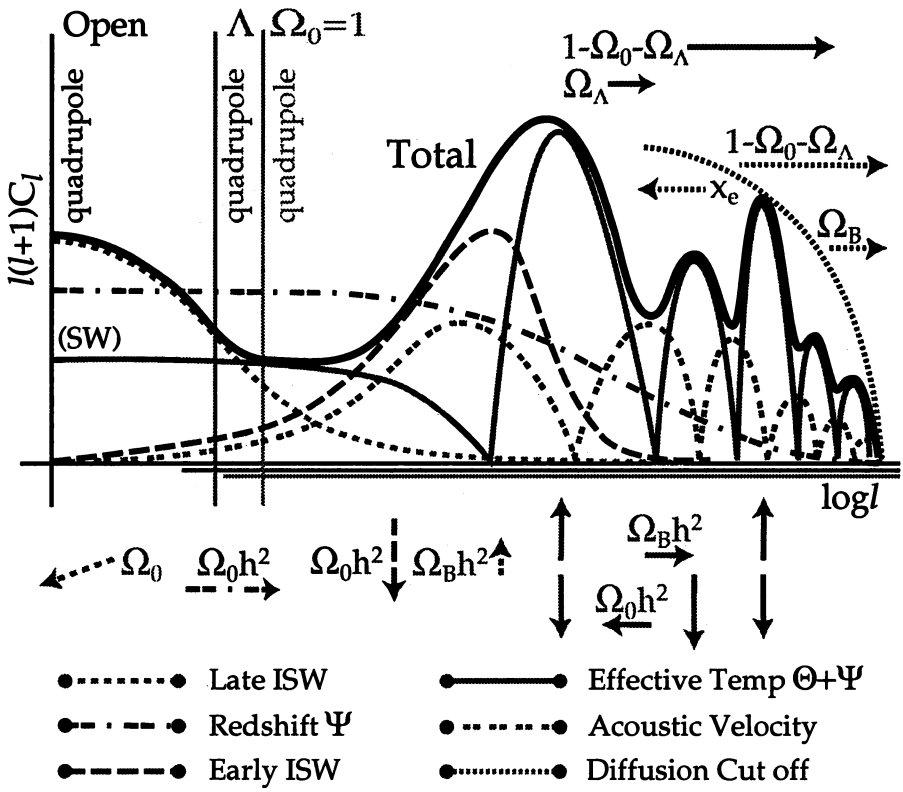

Figure 3. Individual effects on C_ℓ and their dependence on cosmological parameters. This figure is reprinted from Hu et al. (1995).

tail makes the dominant contribution for the $\Omega_0 = 1$ model. On the other hand, there is the late ISW contribution for low density models. As for the Λ model, the ISW effect dominates on large scales. Because this effect has the damping caused by the finite thickness of *gravitational last scattering* (Hu & Sugiyama 1994), it is only significant on very large scales (small ℓ). For the open model, there is another effect, i.e., the cutoff at the curvature scale (Wilson 1983, Sugiyama & Silk 1994, Hu & Sugiyama 1994). Because the fluctuations outside the curvature scale do not contribute on C_ℓ, there is a cutoff on very large scales.

5. Constraints from Observations

It is found that the power spectrum of CMB anisotropies C_ℓ contains rich informations in its shape. On very large scales ($\ell < 50$), C_ℓ's are sensitive

https://doi.org/10.1017/S0074180900132206 Published online by Cambridge University Press

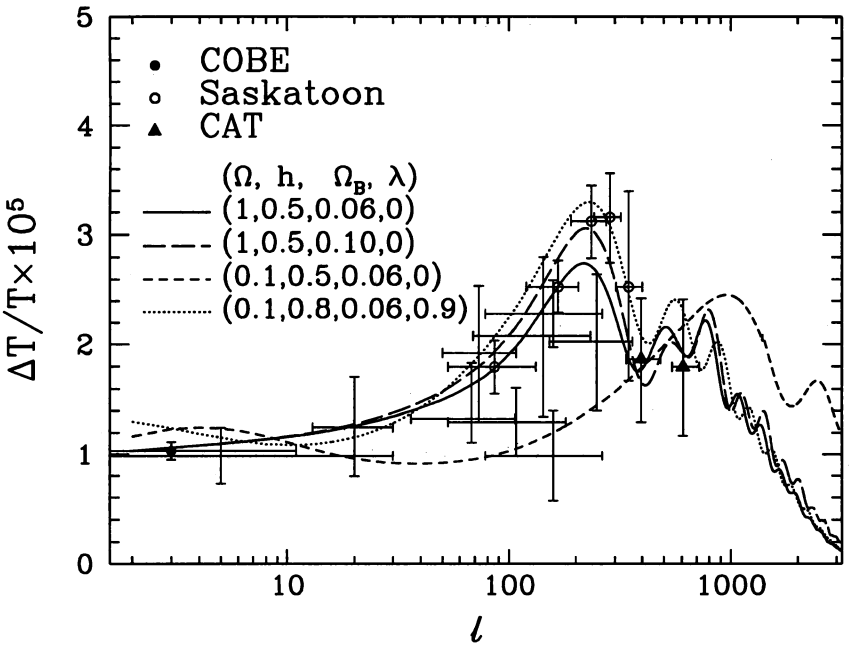

Figure 4. Square root of the CMB power spectrum as a function of multipole ℓ for various cosmological parameters of CDM models together with several recent observations.

to the initial condition of perturbations, Ω_0 and Λ. In fact, we did give an constraint on Λ by using two year COBE DMR data (Bunn & Sugiyama 1995). Employing Bayesian analysis, we got $\Lambda < 0.8$. On scales $50 < \ell < 200$, contributions of the early ISW effect on CMB anisotropies are large. Therefore the shape of C_ℓ in this region is sensitive to $\Omega_0 h^2$. Moreover, if the isocurvature perturbations are considered, the first peak location is around $\ell = 100$. In this case, since the second peak (around $\ell = 300$) is usually higher than the first one, we can easily distinguish it. Finally, if sufficient reionization happens after recombination, a new peak is generated at the place corresponding to the horizon scale of new last scattering surface which is typically $\ell \sim 50$ (Sugiyama, Silk & Vittorio 1993). If there is no peak smaller than this scale, it might be the evidence of the late time reionization. On scales larger than $\ell = 100$, the most prominent figure of C_ℓ which we expect is the existence of high peaks. The location of the first peak will reveal the geometry of the universe. The height and location of peaks tells us about $\Omega_B h^2$ and $\Omega_0 h^2$. The damping scale is mostly sensitive to Ω_B. In near future, we will be able to determine these cosmological parameters out of observations of CMB anisotropies. In figure 3, we summarize all

https://doi.org/10.1017/S0074180900132206 Published online by Cambridge University Press

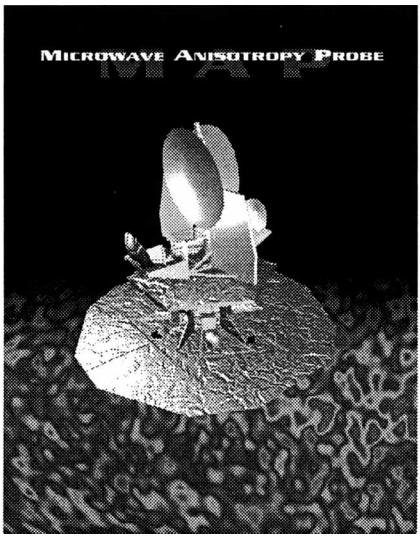

(a)

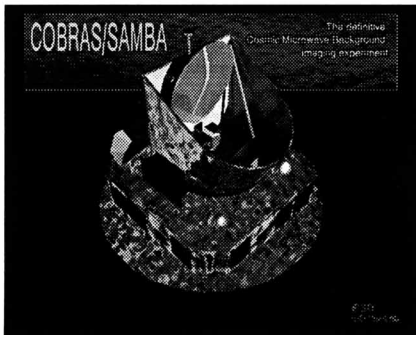

(b)

Figure 5. (a): MAP (Microwave Anisotropy Probe) Satellite. This US mission will measure CMB anisotropies over the full sky. It will be launched in 2000. Five frequency bands from 22 GHz to 90 GHz are taken to remove the signals from the Galaxy. The angular resolution is about a half degree and the sensitivity is 20μK. See http://map.gsfc.nasa.gov for more detailed information. (b): PLANCK satellite. This ESA mission haves 9 bands, 10arcmin resolution instruments which allow to determine the spectrum of CMB anisotropies more precisely. See http://astro.estec.esa.nl/SA-general/Projects/Cobras/cobras.html.

dependence of C_ℓ on various cosmological parameters. In Figure 4, the numerical values of C_ℓ's for several cosmological models with the current status of observations are shown. We might be able to get a rough idea how strong present constraints on model parameters from observations.

6. Concluding Remarks and Future Prospect

The dependence of the power spectrum of CMB anisotropies on cosmological parameters is discussed by using a toy model based on the analogy of a harmonic oscillator. In fact, we are now realizing how powerful CMB anisotropies are to determine the cosmological parameters. Several exciting new observations of CMB anisotropies are being planned. New satellite missions by Europe (PLANCK) and USA (MAP) and long duration flight balloon experiments are discussed (see fig.5). If once we get all (or nearly

https://doi.org/10.1017/S0074180900132206 Published online by Cambridge University Press

all) sky maps with fine resolution ($\sim$ 10arcmin.), we will be able to reconstruct the CMB anisotropy spectrum C_ℓ up to the damping scale. We will soon see the nature of our universe.

References

Bunn, E., & Sugiyama, N. 1995, *Ap.J.*, **446**, 49.
Hu, W., & Sugiyama, N. 1994, *Phys. Rev.* **D50**, 627.
Hu, W., & Sugiyama, N. 1995a, *Ap.J.*, **444**,489.
Hu, W., & Sugiyama, N. 1995b, *Phys. Rev.* **D51**, 2599.
Hu, W., Sugiyama, N. & Silk, J. 1997, *Nature* **386** 37.
Jones, M. et al., 1993, *Nature* **365**, 320.
Kamionkowski, M., Spergel, D. N. & Sugiyama, N. 1994, *Ap.J. Letter*, **426**, L57.
Lyth, D., & Stewart, E.D. 1990, *Phys. Lett.*, **B252**, 336.
Mather, J.C. et al., 1994, *Ap.J.*, **420**,439.
Ratra, B., & Peebles, P.J.E. 1995, *Phys. Rev.* **D52**, 1837.
Sachs, R. K., & Wolfe, A. M. 1967, *Ap.J.*, **147**, 73.
Silk, J. 1968, *Ap.J.*, **151**, 459.
Smoot, G. et al., 1992, *Ap.J. Letter*, **396**, L1.
Sugiyama, N. 1995, *Astrophys. J. Suppl.*, **100**,281.
Sugiyama, N., & Silk, J., 1994, *Phys. Rev. Lett.*, **73**, 509.
Sugiyama, N., Silk, J., & Vittorio, N. 1993, *Ap.J. Letter*, **419**, L1.
Sunyaev, R.A., & Zeldovich, Ya.B. 1970, *Ap. Space Sci.*, **9**, 378.
White, M., Scott, D., & Silk, J. 1993, *ARA&A*, **32**, 319.
Wilson, M. L. 1983, *Ap.J.*, **273**, 2.
Zeldovich, Ya.B., & Sunyaev, R.A. 1969, *Ap. Space Sci.*, **4**, 301.